THE JOURNAL OF BIOLOGICAL CHEMISTRY
Vol. 278, No. 39, Issue of September 26, pp. 37664–37671, 2003
Printed in U.S.A.

Essential Cell Division Protein FtsZ Assembles into One Monomer-thick Ribbons under Conditions Resembling the Crowded Intracellular Environment*

Received for publication, May 19, 2003
Published, JBC Papers in Press, June 14, 2003, DOI 10.1074/jbc.M305230200

José Manuel González‡§, Mercedes Jiménez‡, Marisela Vélez¶‖, Jesús Mingorance, José Manuel Andreu‡, Miguel Vicente**, and Germán Rivas‡ ‡‡**

*From the ‡Centro de Investigaciones Biológicas and the **Centro Nacional de Biotecnología, Consejo Superior de Investigaciones Científicas, and the ¶Instituto Nicolás Cabrera, Facultad de Ciencias, Universidad Autónoma, Madrid E-28040, Spain*

Experimental conditions that simulate the crowded bacterial cytoplasmic environment have been used to study the assembly of the essential cell division protein FtsZ from *Escherichia coli*. In solutions containing a suitable concentration of physiological osmolytes, macromolecular crowding promotes the GTP-dependent assembly of FtsZ into dynamic two-dimensional polymers that disassemble upon GTP depletion. Atomic force microscopy reveals that these FtsZ polymers adopt the shape of ribbons that are one subunit thick. When compared with the FtsZ filaments observed *in vitro* in the absence of crowding, the ribbons show a lag in the GTPase activity and a decrease in the GTPase rate and in the rate of GTP exchange within the polymer. We propose that, in the crowded bacterial cytoplasm under assembly-promoting conditions, the FtsZ filaments tend to align forming dynamic ribbon polymers. *In vivo* these ribbons would fit into the Z-ring even in the absence of other interactions. Therefore, the presence of mechanisms to prevent the spontaneous assembly of the Z-ring in non-dividing cells must be invoked.

The FtsZ protein is conserved in most of the prokaryotic organisms and several organelles and plays a central role in microbial and organelle division forming a ring at the division site (1, 2). It is structurally related to the eukaryotic cytoskeletal tubulin (3, 4), binds guanine nucleotides, and has GTPase activity (5–7). In the presence of GDP, the FtsZ monomers undergo a reversible non-cooperative magnesium-linked association to form linear oligomers (8, 9), whereas in the presence of GTP, a variety of polymers are formed *in vitro* (10–16; for a recent review see Ref. 17).

It is assumed that FtsZ association and assembly reactions studied *in vitro* should play an important role in bacterial cell division *in vivo*, but the correlation between these *in vivo* and *in vitro* processes is not known. Moreover the assay conditions used *in vitro* differ substantially from the bacterial cytoplasm where FtsZ is located and functions. Most of the experimental work performed *in vitro* is done under solution conditions in which the total concentration of macromolecules is low (1 or less), whereas the estimated concentration of proteins and nucleic acids in the highly volume-occupied ("crowded") bacterial interior is on the order of 300–400 g/liter (18, 19). Excluded volume effects in macromolecular crowded environments have significant consequences on the energetics and dynamics of functional assembly processes (20, 21). Macromolecular crowding has been described to favor several assembly processes of actin and tubulin, such as the rate and extent of polymerization and their organization into more complex structures (22–24). In the case of FtsZ, it has been previously shown that crowding facilitates the formation of magnesium-dependent GDP-FtsZ oligomers (25).

We have investigated the effects of macromolecular crowding upon the more complex and physiologically relevant FtsZ assembly processes taking place in the presence of GTP, which is the most abundant form of the nucleotide in the cell. By means of analytical centrifugation, light scattering, optical, electron, and atomic force microscopy and assays of biochemical activity performed in solutions containing a suitable content of the main physiological osmolytes (see "Materials and Methods" (18)), we have found that high concentrations of unrelated macromolecules, resembling the crowded *Escherichia coli* cytoplasm, favor the formation of two-dimensional FtsZ polymer arrays (ribbons). This self-organization process, which is GTP-dependent, retards significantly the FtsZ GTPase activity, the polymer assembly/disassembly dynamics, and the nucleotide exchange within the polymer, when compared with the same parameters measured in the FtsZ filaments formed in dilute solutions. We conclude that in the bacterial interior FtsZ may tend to spontaneously arrange into one-subunit-thick ribbons and suggest, that in the non-dividing cell, their formation must be modulated by other mechanisms that regulate Z-ring assembly.

MATERIALS AND METHODS

Reagents—Guanine nucleotides, GDP and GTP, were from Sigma and Roche Molecular Biochemicals, respectively. The nucleotide analog GMPCPP,[1] which hydrolyzes more slowly than GTP, was purchased from Jena Bioscience. Fluorescein 5′-isothiocyanate (FITC) was from Molecular Probes Inc. Other analytical grade chemicals were from

* This work was supported in part by Grants BIO99-0859-C03-03 and BMC2002-04617-C02-01 (to G. R.), BMC2002-04617-C02-02 (to M. Vé.), BIO2000-0451-P4-02 (to M. Vi.), and BIO99-0859-C03-02 and BIO2002-03665 (to J. M. A.), all from the Spanish Ministry of Science and Technology (MCyT), and by the Programa de Grupos Estratégicos of the Madrid Government (to J. M. A. and G. R.). The costs of publication of this article were defrayed in part by the payment of page charges. This article must therefore be hereby marked "*advertisement*" in accordance with 18 U.S.C. Section 1734 solely to indicate this fact.

§ Supported by an MCyT fellowship.

‖ An MCyT Ramón y Cajal fellow.

‡‡ To whom correspondence should be addressed: Centro de Investigaciones Biológicas, CSIC, Ramiro de Maeztu 9, E-28040 Madrid, Spain. Tel.: 34-91-534-6623; Fax: 34-91-562-7518; E-mail: grivas@cib.csic.es.

[1] The abbreviations used are: GMPCPP, guanosine-5′-[(α,β)-methyleno]triphosphate; AFM, atomic force microscopy; FITC, fluorescein isothiocyanate; GFP, green fluorescent protein.

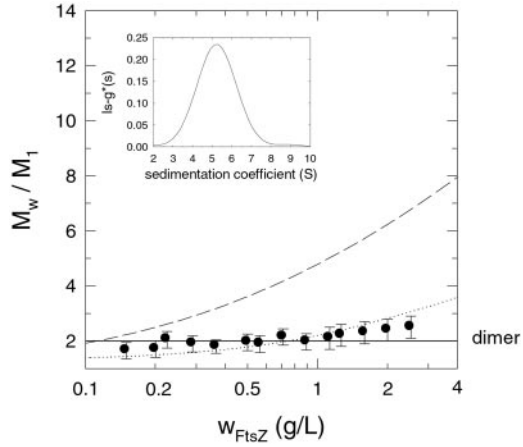

FIG. 1. **Self-association of *E. coli* GDP-FtsZ in physiological buffer measured by analytical ultracentrifugation.** The protein FtsZ from *E. coli* was equilibrated in KGA buffer with 50 μM GDP, and its state of association was analyzed by means of analytical centrifugation (sedimentation equilibrium and velocity) as described under "Materials and Methods." The *closed circles* show the sedimentation equilibrium data obtained at 15,000 rpm and 20 °C. The *dashed line* shows the corresponding best fit to the Mg^{2+}-linked indefinite self-association model described in Ref. 8 in Tris-KCl, pH 7.4, buffer with 5 mM Mg^{2+} ($K \cong 10^6$ M^{-1}). The *dotted line* shows the best fit for an isodesmic self-association from FtsZ monomers ($K = 6 \times 10^3$ M^{-1}). The *inset* shows the sedimentation coefficient distribution for 1.0 g/liter FtsZ after sedimentation velocity at 60,000 rpm and 20 °C.

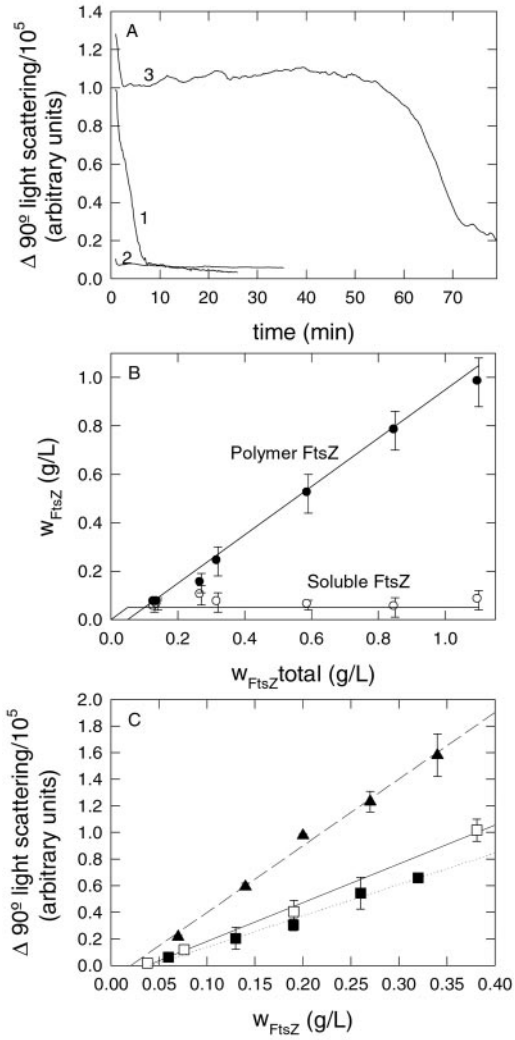

FIG. 2. **FtsZ assembly in physiological buffer analyzed by scattering and sedimentation assays.** *A*, FtsZ (0.5 g/liter) was incubated at 30 °C in KGA buffer without regeneration system (*curve 1*) or with a GTP-regenerating system, as described in the text (*curve 3*). GTP was added to a concentration of 2 mM (corresponding to the increase in the scattering signal), and the polymerization was followed by 90° light scattering as described under "Materials and Methods." The corresponding scattering profile upon addition of GDP instead of GTP is shown in *curve 2*. *B* and *C*, Determination of the apparent critical concentration for FtsZ filament formation (C_{fil}). *B*, high speed centrifugation assay. The assembly of FtsZ was triggered upon addition of 2 mM GTP to FtsZ in KGA buffer with the GTP-regenerating system. The soluble (*open circles*) and polymerized (*closed circles*) FtsZ were separated by sedimentation in a tabletop ultracentrifuge as described in the text. Both protein species were measured with a colorimetric assay. The *solid lines* represent the best fit to a first-order transition model (C_{fil} = 0.05 g/liter). *C*, dependence of the 90° light scattering increment upon FtsZ concentration after the addition of GTP, without (*open squares*) or with (*closed squares*) a GTP-regenerating system, or GMPCPP (*closed triangles*).

Merck or Sigma. Macromolecular crowders (dextran T70 and Ficoll 70, both with average molar weights of 70,000) were obtained commercially from Amersham Biosciences. They were used without further purification after extensive dialysis against the corresponding working buffer. The final concentration of the equilibrated stock solutions of crowder was determined refractometrically using 0.134 and 0.140 ml g^{-1} as the specific refractive index increments at 620 nm of Ficoll and dextran, respectively (26).

Protein Purification—E. coli FtsZ was purified by the calcium-induced precipitation method following the procedure described previously (8). The protein concentration was measured using the BCA assay (Pierce), with spectrophotometrically calibrated FtsZ standards (see Ref. 8) and bovine serum albumin as secondary standard, which gave a 0.80 ± 0.03 color ratio of FtsZ/albumin (in agreement with Ref. 27).

Physiological Buffer and Enzymatic GTP-regenerating System—Most of the *in vitro* studies of FtsZ (reviewed in Refs. 17 and 28; see also Refs. 12–14) have been carried out in chloride-containing buffers at potassium concentrations that are at the lower end or below the physiological range of this cation. Moreover, many of these studies have been done at slightly acidic pH (6.5). These buffers do not mimic the main intracellular ionic environment of the bacterial interior. For example, chloride is present only at very low concentration in the cytoplasm of *E. coli*. At moderate to high external osmolarities, potassium (ranging from 0.2 to 0.9 M) and glutamate (from 0.03 to 0.2 M) ions are concentrated in the cytoplasm of *E. coli* to prevent dehydration and maintain turgor pressure (18). It has been reported that several of these physiological osmolytes (*i.e.* glutamate) are modulators of non-covalent DNA-protein interactions *in vitro* (18, 29).

Therefore, most of the experiments described in this work were done in KGA buffer (25 mM Hepes/acetate, pH 7.4, plus 100 mM potassium glutamate, 300 mM potassium acetate, and 5 mM magnesium acetate), which contains the major osmolyte species present in bacterial cytoplasm, supplemented with guanine nucleotides as noted. This buffer with a high potassium content, which increases the intrinsic GTPase activity of *E. coli* FtsZ and therefore the rate of disassembly of FtsZ filaments (for a recent review see Ref. 28), makes it difficult to get stable FtsZ polymers during the time-scale (>10 min) of most of the experiments performed in this work (mainly those done in the absence of crowding agents, see below). In these experiments the GTP was regenerated by adding to the solution an enzymatic regeneration system (1 unit/ml acetate kinase plus 15 mM acetyl phosphate, both from Sigma), as adapted from tubulin/microtubules studies (30). Under these conditions FtsZ polymers were stable in solution during at least 1 h at 30 °C (at 1 g/liter FtsZ). Higher acetyl phosphate concentrations (>50 mM) interfered with FtsZ filament formation (three-dimensional polymer bundles are favored; see AFM results) and with negative staining electron microscopy. Alternatively, in some experiments GTP was replaced by GMPCPP, a GTP analog more slowly hydrolyzable (15).

FITC Labeling of FtsZ—The labeling of FtsZ with the fluorescent dye fluorescein isothiocyanate (FITC) was carried out as follows. FtsZ (4–6 g/liter) was dialyzed against 20 mM Hepes/HCl, pH 8.0, buffer with 50 mM KCl, 5 mM $MgCl_2$, and 1 mM EDTA. To minimize perturbations on FtsZ association/assembly properties due to the labeling, the protein was previously polymerized at 30 °C upon addition of 20 mM calcium and 2 mM GTP (8). To this preparation a 40-fold excess of FITC was added, and the mixture was incubated for 15 min at 30 °C. The precipitate was resuspended in cold in 50 mM Tris/HCl, pH 7.4, buffer with 100 mM KCl, and the free FITC was removed by gel filtration. The

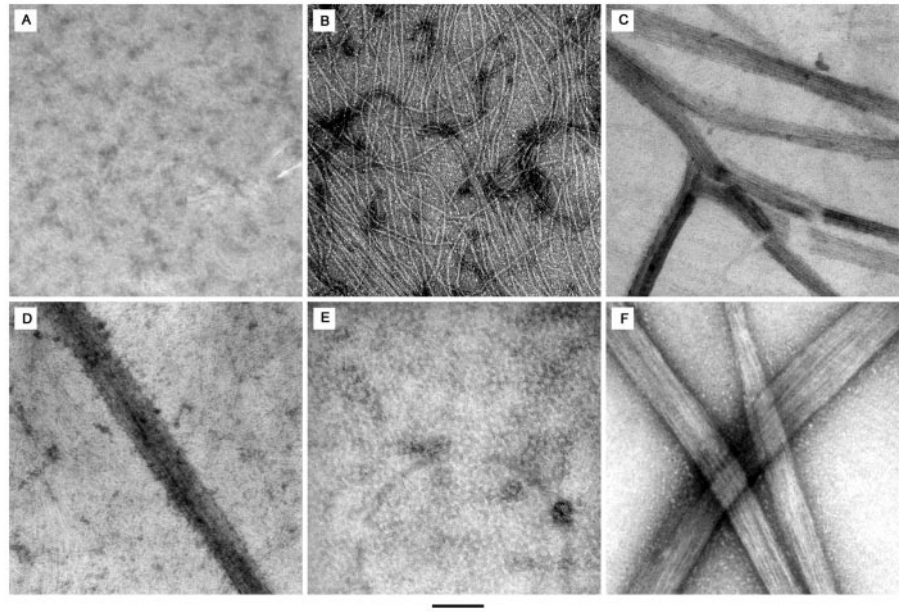

FIG. 3. **Electron microscopy analysis of FtsZ assembly in the absence and in the presence of macromolecular crowders.** *Top row*, *left-hand side*: electron micrograph of negative stained FtsZ (1.0 g/liter) samples in 50 mM Tris-HCl, 100 mM NaCl, pH 7.4, buffer (which does not contain potassium and does not promote FtsZ assembly, see Ref. 13) plus 1 mM GTP and 200 g/liter Ficoll 70. The other electron micrographs correspond to negatively stained FtsZ samples in KGA buffer. *Top row*, *center*: FtsZ (0.5 g/liter) plus 1 mM GTP. *Top row*, *right-hand side*: FtsZ (0.2 g/liter) plus 2 mM GTP and 220 g/liter Ficoll 70. *Bottom row*, *left-hand side*: FtsZ (0.1 g/liter) plus 2 mM GTP and 200 g/liter dextran T70. *Bottom row*, *center*: FtsZ (0.5 g/liter) plus 0.5 mM GTP and 200 g/liter Ficoll 70 after 1-h incubation at 30 °C. *Bottom row*, *right-hand side*: FtsZ (0.5 g/liter) plus 0.1 mM GMPCPP and 200 g/liter Ficoll 70. In all cases, the *bar scale* is 100 nm.

precipitation of FtsZ was reversible, and the degree of labeling was 0.9 ± 0.2 mol of FITC per mol of FtsZ.

Analytical Centrifugation—The sedimentation equilibrium and sedimentation velocity experiments in the presence of low concentrations of nucleotide (<0.1 mM) were performed in a Beckman XL-A (Beckman-Coulter) essentially as described in a previous study (8). The sedimentation coefficient distributions were calculated by least-squares boundary modeling of sedimentation velocity data using the ls-g*(s) method (31) as implemented in the SEDFIT program.

FtsZ Assembly in the Absence of Macromolecular Crowders: 90° Scattering and High Speed Centrifugation Assays—The formation of FtsZ polymers in the absence of crowding agents was followed by light scattering at 90° (14) using a Jobin Yvon Fluorolog-3 spectrofluorometer. Excitation and emission wavelengths were set to 350 nm, with slit widths of 0.5 nm (excitation) and 1 nm (emission). All reactions were performed at 30 °C. FtsZ (0.1–1.0 g/liter) was incubated in KGA buffer (with or without an enzymatic GTP-regenerating system) in a fluorometer cuvette. After 5 min of equilibration, 1 mM GTP (or 0.1 mM GMPCPP) was added, and the reactions were monitored. The formation of FtsZ filaments was also followed by high speed centrifugation during 15 min at 240,000 × *g* and 30 °C using the TLA100 rotor in an Optima MAX tabletop ultracentrifuge (Beckman-Coulter Inc.).

FtsZ Assembly in the Presence of Macromolecular Crowders: Low Speed Centrifugation, 90° Scattering, and Turbidity Assays—The relatively low viscosity and density of Ficoll 70 (32), which reduces the apparent sedimentation coefficients of FtsZ species by a factor of five in 200 g/liter Ficoll 70 solutions, permits the use of a low speed sedimentation method to assay the formation of FtsZ ribbon polymers in the presence of this crowder agent. 100 μl of a given concentration of FtsZ were centrifuged at low speed (25,000 × *g* for 10 min at 30 °C) using the TLA100 rotor in an Optima MAX ultracentrifuge (Beckman-Coulter Inc.). The entire supernatant and the pellet were carefully removed, and the protein content was measured in both fractions as well as in the original samples (controls). The supernatant fraction only contains soluble protein and filaments but no ribbons as judged by electron microscopy; the pellet contained mainly the FtsZ ribbons. Control assembly experiments in the absence of crowders showed that under these sedimentation conditions >95% of FtsZ filaments were recovered in the soluble fraction. Therefore this assay discriminates between filaments and ribbons in a quantitative manner.

The crowding-induced FtsZ ribbons were also monitored by two scattering assays: 90° light scattering (as described above), which detected both the FtsZ filaments and ribbon polymers, and turbidity (33) in an Ultrospec 3000*pro* UV-visible spectrophotometer (Amersham Biosciences). The latter is also a specific method for monitoring FtsZ ribbons (because of their size) in the presence of macromolecular crowders, but it does not detect the assembly/disassembly of FtsZ filaments (8).

Electron Microscopy—The FtsZ polymers (protein concentration ranging from 0.05 to 1 g/liter), in the absence or in the presence of high concentrations of macromolecular crowders (dextran T70 or Ficoll 70), were visualized by electron microscopy after negative staining with 2% uranyl acetate, using either a JEOL-1200 or a LEO 910 electron microscope.

Atomic Force Microscopy—AFM images were taken with an Atomic Force Microscope (Nonatec Electrónica, Madrid, Spain) operated in the jump mode (34). The scanning piezo measurement was calibrated using silicon calibrating gratings. Silicon nitride tips (DI instruments) with constant force of 0.2 N7M were used. A drop of the solution with the FtsZ polymers (formed upon addition of 0.1 mM GMPCPP to the protein in KGA buffer with 100–200 g/liter Ficoll) was incubated over freshly cleaved circular pieces of mica glued onto a Teflon surface, and, after a few minutes, the samples were extensively washed with working buffer and allowed to dry for 15 min under a stream of air.

Optical Microscopy—The FtsZ samples labeled with the fluorescent dye FITC were placed directly onto a glass slide, and the polymers were visualized using a Zeiss Axioscope epifluorescence microscope equipped with the FITC filter set and 40×/63×/100× oil immersion objectives. Images were captured with a Photometrics charge-coupled device camera.

Other Analytical Procedures—The total nucleotide content of the protein preparations was measured spectrophotometrically after protein extraction with perchloric acid (8, 35). Specific nucleotides were measured by means of ionic-pair high-performance liquid chromatography (35). The GTPase turnover rate was determined by measuring released inorganic phosphate using the malachite green-molybdate reagent (36, 37). The incorporation of GTP into FtsZ polymers was measured by a nitrocellulose filter-binding assay using [γ-^{32}P]GTP, as described in a previous study (13).

RESULTS

FtsZ in Its GDP-bound State in Physiological Buffer Has a Weak Tendency to Oligomerize—We have studied the influence of physiological concentrations of osmolytes present in the *E. coli* cytoplasm (KGA buffer; see "Materials and Methods") on the magnesium-induced oligomerization of *E. coli* GDP-FtsZ. In a previous study, the behavior of GDP-FtsZ in a Tris, pH 7.4, 50 mM KCl buffer was best described by a Mg^{2+}-linked indefinite self-association of FtsZ monomers, with a weakening of the monomer-monomer interaction upon increasing ionic strength (8). Analytical ultracentrifugation experiments (sedimentation equilibrium and velocity) were carried out in the presence of GDP. Fig. 1 shows the dependence of the state of association of FtsZ in KGA buffer upon protein concentration. The results indicate that the predominant species over the concentration range studied (0.1–2.5 g/liter) has an average size corresponding to an FtsZ dimer, with a trend to form monomer and higher

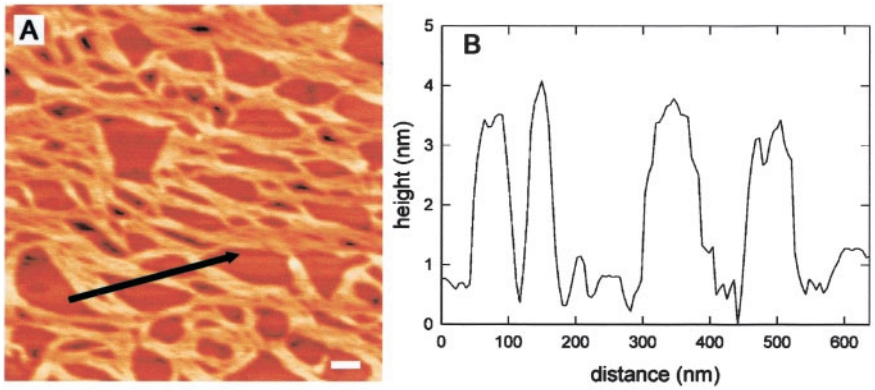

FIG. 4. **Atomic force microscopy analysis of crowding-induced FtsZ assembly.** *A*, AFM images of FtsZ polymers induced upon addition of 0.1 mM GMPCPP in KGA buffer with 200 g/liter Ficoll. The height scale was 6 nm. The *white bar* represents 100 nm. *B*, distance profile of a selected region (*black bar*) of the image shown in *A*. The *vertical axis* corresponds to the thickness of the structures observed in *A*, whereas the *horizontal axis* indicates the distance (related with the polymer width) over the selected segment.

oligomers at, respectively, decreasing or increasing protein concentrations. In the *inset* of Fig. 1 the sedimentation velocity ls-g*(s) distribution of FtsZ (1 g/liter) in KGA buffer is plotted. This sedimentation coefficient distribution corresponds to a symmetrical peak with an average sedimentation coefficient of 5.2 S, which is compatible with an average FtsZ dimer (8). These data are in agreement with a previous report showing that, over a broad range of protein concentrations, increasing the ionic strength from 50 to 500 mM KCl lowers the average molar mass and sedimentation coefficient of GDP-FtsZ (8). The weak dependence upon protein concentration of the FtsZ self-association in KGA buffer precludes a complete quantitative analysis. The isodesmic association that previously best described the formation of FtsZ oligomers from monomers (*dashed line* in Fig. 1; see Ref. 8) may also apply in the present work (performed in KGA buffer) but with a much weaker association constant (*dotted line* in Fig. 1). We conclude that in solutions that reproduce the main intracellular osmolarity, FtsZ in its GDP-bound state has a weak tendency to form high order oligomers.

FtsZ in the Presence of GTP in Physiological Buffer Assembles into Dynamic Filaments—At 30 °C in KGA buffer FtsZ polymers formed quickly upon addition of 1 mM GTP as monitored by 90° light scattering (Fig. 2*A*). Under the same conditions addition of GDP failed to induce polymerization (Fig. 2*A*). Given the high concentration of potassium ions in the buffer the GTPase activity of FtsZ is activated, causing the FtsZ polymers to rapidly disassemble following GTP consumption, as reported in other publications (8, 14, 38). To overcome the polymer instability, when needed, an enzymatic GTP-regenerating system was added to the preparations (see "Materials and Methods"). Under these conditions, the polymers at 1 g/liter protein were stable for 1 h (Fig. 2*A*) and could be visualized in electron micrographs of negatively stained preparations as filaments of variable length and curvature with a thickness of 5–6 nm (Fig. 3, *top row*, *center*). FtsZ filaments with a thickness of 6–8 nm were also found upon incubation of the protein with GMPCPP, an analog of GTP that is hydrolyzed by FtsZ much more slowly than GTP (not shown).

The soluble and polymerized fractions of FtsZ formed in the presence of the GTP-regenerating system were separated by high speed centrifugation and quantitated (see "Materials and Methods"). Filament formation depended on the concentration of FtsZ showing an apparent critical concentration for filament formation (C_{fil}) of 0.05 ± 0.01 g/liter (1.25 μM, Fig. 2*B*). Similar samples were analyzed by 90° light scattering resulting in a very similar value for C_{fil} (0.04 ± 0.01 g/liter; Fig. 2*C*, *closed squares*). Light scattering analysis were also performed in the absence of the GTP-regenerating system, and the C_{fil} value determined using the initial scattering increments was practically identical to that obtained in the presence of the GTP-regenerating system (Fig. 2*C*, *open squares*). The experimental value found for C_{fil} when GTP was replaced by GMPCPP was slightly lower (0.03 ± 0.01 g/liter; Fig. 2*C*, *closed triangles*). These results indicate that FtsZ filament formation occurs in a cooperative fashion (33). The functioning of a cooperative mechanism of FtsZ polymerization has been proposed as well by

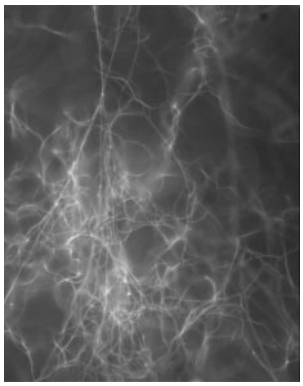

FIG. 5. **Crowding-induced formation of FtsZ polymers as monitored by optical microscopy.** A mixture of labeled (0.05 g/liter) and unlabeled (0.5 g/liter) FtsZ in KGA buffer was incubated with 2 mM GTP, in the presence of 150 g/liter of Ficoll (×40).

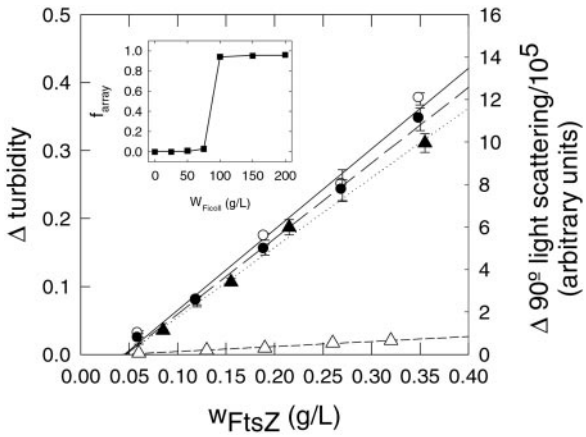

FIG. 6. **Determination of the apparent critical concentration for the formation of FtsZ ribbons (C_{ribbon}).** Dependence on protein concentration of the turbidity signal due to the formation of FtsZ ribbons upon addition of GTP to FtsZ in KGA buffer with GTP-regeneration system and 100 g/liter (*closed circles*) or 200 g/liter (*open circles*) of Ficoll 70. The *triangles* show the corresponding 90° light scattering profiles with (*closed symbols*; signal is related to ribbon formation) or without (*open symbols*; filament formation) 200 g/liter Ficoll 70. *Inset*, dependence of the fractional abundance of FtsZ ribbons upon Ficoll concentration, as measured by low speed centrifugation (total protein concentration was 1 g/liter).

others (14, 38–40).[2] In contrast, in the presence of GDP most of the FtsZ protein (over 98%) was recovered in the soluble fraction as would be expected if the dimer were the most abundant form of the GDP-bound FtsZ in solution (see above, Fig. 1).

Macromolecular Crowding Favors the GTP-dependent Formation of Dynamic FtsZ Polymers—The bacterial cytoplasm is a highly crowded environment, a condition that has not been analyzed when studying the formation of FtsZ filaments. To approximate the intracellular conditions we have studied the polymerization of FtsZ in the presence of high concentrations of inert macromolecular crowders (Ficoll or dextran, both with an average molar weight of 70,000, see "Materials and Methods"), as has been used for the study of other systems (20, 21).

We analyzed first the effect of crowding agents in the absence of potassium ions, a condition under which FtsZ has been found to bind GTP but does not polymerize (13). FtsZ polymers were not observed by negative staining electron microscopy even in the presence of high concentrations (100–200 g/liter) of macromolecular crowders (Fig. 3, *top row*, *left-hand side*). This result was also confirmed by low speed centrifugation and turbidity assays (not shown).

As described above in the presence of potassium ions (KGA buffer) FtsZ predominantly formed filaments upon addition of GTP or GMPCPP (Fig. 3, *top row*, *center*). The appearance of the FtsZ polymers, observed in electron micrographs after negative staining, was drastically modified in the presence of high concentrations of dextran or Ficoll. Addition of 200 g/liter of Ficoll 70 resulted in the formation of polymers, some of them interconnected, with a width of 40–100 nm (Fig. 3, *top row*, *right-hand side*). Considering that the dimensions of the FtsZ monomer are 4–5 nm (3), these polymers would correspond to a width of 8–25 single protofilaments. Similar results were obtained when 200 g/liter dextran was used to simulate crowding (Fig. 3, *bottom row*, *left-hand side*). These polymers were also observed when the incubation in KGA buffer was done in the presence of 0.1 mM GMPCPP instead of GTP (Fig. 3, *bottom row*, *right-hand side*). However, they disappeared, unless GTP was regenerated by a GTP-regenerating system, when the incubation time exceeded 1 h, suggesting that they are dynamic structures (Fig. 3, *bottom row*, *center*). Similarly, although the self-association of GDP-FtsZ into short oligomers is enhanced by macromolecular crowders at lower ionic strengths (8, 25), the addition of GDP failed to promote the formation of FtsZ polymers both at lower ionic strengths and in KGA buffer (not shown).

The FtsZ Polymers Formed in the Presence of Crowding Agents Are One Subunit-thick Ribbons—Atomic force microscopy (AFM) images show that the width of the FtsZ polymers induced by crowding agents is 40–100 nm, corresponding to the lateral association of 8–25 single protofilaments, and their thickness is 3–4 nm (Fig. 4). This size is compatible with two-dimensional structures with a thickness of one protofilament. We propose therefore that the FtsZ polymers induced by crowding agents are ribbons. Their observed width is similar to the width of the negatively stained polymers observed by electron microscopy (Fig. 3, *bottom row*, *right-hand side*). Moreover, the interconnection between filaments found in the electron micrographs was also observed in the AFM preparations.

The FtsZ ribbons induced by crowding agents were large enough to be observed under the optical microscope when fluorescently (FITC)-labeled FtsZ was used (Fig. 5). In the absence of crowders, fluorescently labeled FtsZ did not form any structure that could be visualized under the optical microscope (not shown).

[2] S. Huecas and J. M. Andreu, submitted manuscript.

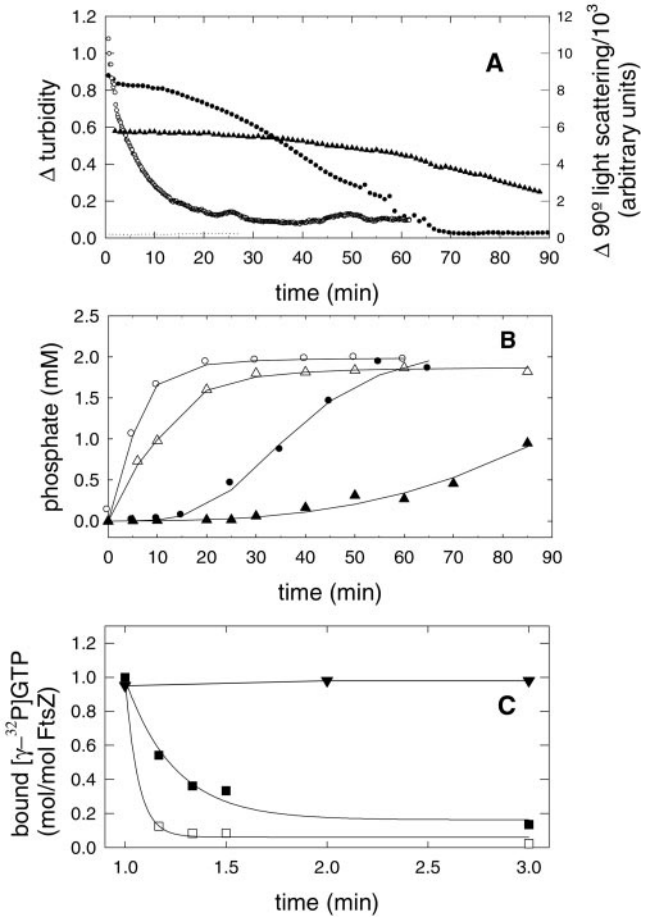

FIG. 7. **Effect of crowding on the assembly/disassembly dynamics, GTPase turnover, and nucleotide exchange of FtsZ polymers.** *A*, the *open circles* show the 90° light scattering profile of FtsZ polymers (2.0 g/liter) upon addition of 2 mM GTP in KGA buffer at 30 °C without adding a macromolecular crowder. Turbidity profiles of FtsZ in KGA buffer with 200 g/liter Ficoll 70, upon addition of either 2 mM GTP (*solid circles*: 2.0 g/liter FtsZ; *closed triangles*: 0.2 g/liter; signal is ×10 for comparison purposes) or GDP (*dotted line*, 2 g/liter FtsZ). *B*, time dependence of the GTPase activity of FtsZ (2.0 g/liter). *Open symbols* correspond to 2 g/liter (*circles*) and 0.2 g/liter (*triangles*) FtsZ in the absence of macromolecular crowders. *Closed symbols* correspond to FtsZ samples in the presence of 200 g/liter Ficoll 70. *C*, nucleotide exchange of FtsZ polymers in the absence (*open squares*) and in the presence (*closed squares*) of 150 g/liter Ficoll. The polymerization was triggered by adding 0.1 mM [γ-^{32}P]GTP to FtsZ (0.5 g/liter) in KGA buffer. After 1 min at 30 °C, unlabeled GTP was added to the reaction mixtures (1 mM nucleotide final concentration), and the amount of radioactive nucleotide bound to the protein was measured using a nitrocellulose filter binding assay. *Closed inverted triangles* represent control experiments without adding unlabeled GTP. The *solid lines* represent the best-fit first-order decay functions.

Crowding Promotes the Formation of FtsZ Ribbons from Preformed FtsZ Filaments—Formation of FtsZ filaments does not produce significant increases in turbidity (8). Turbidity measurement was used, therefore, to monitor the formation of the FtsZ ribbons as a function of protein concentration in the presence of Ficoll 70 (Fig. 6). In the presence of a GTP-regenerating system or GMPCPP at crowder concentrations ranging between 100 and 200 g/liter, the turbidity increase caused by the formation of FtsZ ribbons was found to be directly proportional but to remain stable for times inversely related to the concentration of FtsZ (30 min at 2 g/liter and over 1 h at 0.2 g/liter) (Fig. 6). From the *x*-axis intercept of this plot the apparent critical concentration for FtsZ ribbon formation (C_{ribbon}) in the presence of Ficoll was determined. The value of C_{ribbon}

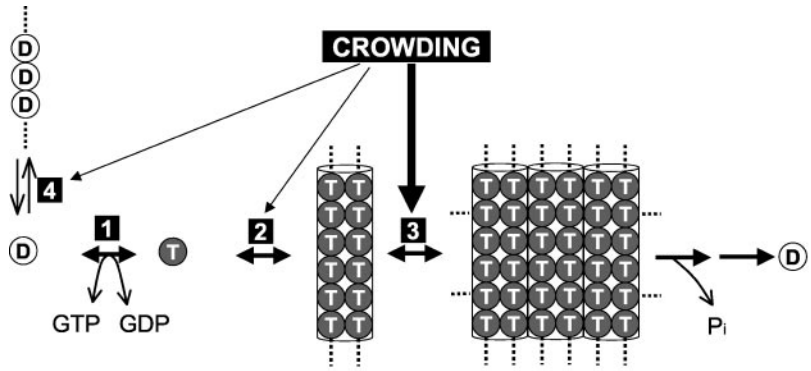

FIG. 8. **Model for the assembly of FtsZ under conditions resembling the crowded bacterial interior.** This *schematic* summarizes the FtsZ assembly reactions taking place in the presence of GTP, both in the absence and in the presence of macromolecular crowders, characterized in this work: the nucleotide exchange in soluble FtsZ (*reaction 1*), the cooperative formation of FtsZ filaments (*reaction 2*), and the assembly into ribbons (*reaction 3*). For simplicity the soluble FtsZ species are represented as *single beads*, although in KGA buffer they are more likely to be dimers. *Reaction 4* shows the magnesium-linked oligomerization of FtsZ in its GDP state at low ionic strength as previously studied (8, 25) (see Fig. 1). Macromolecular crowding plays a more prominent role in enhancing the assembly reaction in which the volume occupied by the final FtsZ product is lower, and therefore the decrease in the amount of excluded volume is larger (*reaction 3*). Our results suggest that the main FtsZ species present in the crowded bacterial interior are soluble GTP-FtsZ and ribbons. *In vivo* the Z-ring may assemble from the FtsZ ribbons requiring no additional interactions, whereas, on the other hand, the existence of mechanisms to prevent the spontaneous Z-ring assembly in non-dividing cells has to be invoked.

was 0.05 ± 0.01 g/liter, both at 200 and 100 g/liter Ficoll (*circles* in Fig. 6). Low speed sedimentation assay and 90° light scattering (see "Materials and Methods") also yield a similar value of 0.06 ± 0.02 g/liter at 200 g/liter Ficoll (Fig. 6). These values of C_{ribbon} were almost identical to the values of C_{fil} determined in the absence of macromolecular crowders (see above and Fig. 2*B*).

Using several independent assays (Figs. 2 and 6) we have determined that the apparent critical concentration for the formation of FtsZ ribbons (C_{ribbon}) in the presence of macromolecular crowders is similar to the value of C_{fil} (the corresponding critical concentration for filament formation) measured in the absence of crowders. These observations indicate that, within the *E. coli* physiological FtsZ concentration range (0.1-1.0 g/liter (12, 41)), macromolecular crowding, rather than favoring the assembly of FtsZ into filaments (see *reaction 2* in Fig. 8 below), promotes the alignment of FtsZ filaments into ribbons (*reaction 3* in Fig. 8). As has been described for tubulin and actin polymerization (22, 24)), and accordingly to excluded volume theory (42–44), cooperative FtsZ filament formation must also be enhanced in a crowded media due to the increase in the local FtsZ concentration in the non-excluded volume (chemical activity). The possible enhancing effect of crowding on filament formation remains nevertheless hidden, first because even in the absence of crowders they should already be present, as is indicated by the rather low value of C_{fil} measured under these conditions (Fig. 2), and, moreover, because the simultaneous effect of excluded volume on ribbon formation is larger.

From the results obtained in both the absence of potassium ions and presence of crowders shown in Fig. 3 (*top row*, *left-hand side*), we conclude that, under these conditions, in which filaments cannot be formed, there is no further assembly of FtsZ into higher order structures. When filaments can be formed, assembly into ribbons follows sharply upon the addition of sufficient concentrations of crowder. This is derived from observations (*inset* of Fig. 6) indicating that the formation of FtsZ ribbons at a fixed protein concentration (1 g/liter), well above the critical concentration for filament formation (0.05 g/liter), undergoes a sharp transition as evidenced by low speed sedimentation assays at concentrations of Ficoll near 100 g/liter. Although FtsZ remains as filaments and does not form ribbons below this concentration of crowder, nearly 95% of FtsZ is found as ribbons when the crowder concentration is higher.

Macromolecular Crowding Retards the Dynamics of the FtsZ Polymer, the GTP Hydrolysis, and the Rate of Nucleotide Exchange—In the presence of high concentrations of macromolecular crowders the FtsZ ribbons, although more stable than the FtsZ filaments, were also found to be dynamic (Fig. 3). It has been previously reported that high concentrations of calcium (in the millimolar range) favor the formation of dynamic FtsZ polymer networks (16). This assembly reaction is GTP-dependent and alters considerably the polymer dynamics. We wanted to investigate the dynamics of the crowding-induced ribbons under conditions more similar to the bacterial cytoplasm. To characterize further the dynamic behavior of FtsZ ribbons, an experiment to measure the effect of the crowder on the disassembly of FtsZ ribbons in the presence of GTP was done. As shown by the turbidity measurements in Fig. 7*A* (*closed circles*), macromolecular crowding stabilized the FtsZ ribbons. On the other hand, the FtsZ filaments, as monitored by 90° light scattering, rapidly disassembled in the absence of crowding (*open circles*). The ribbon was even more stable at low FtsZ concentrations (0.2 g/liter) (Fig. 7*A*, *closed triangles*).

The FtsZ GTPase activity of ribbons induced by either Ficoll (Fig. 7*B*, *closed circles*) or dextran (not shown), when compared with FtsZ filaments (*open circles*), was substantially retarded, resulting in a decreased GTPase turnover. As expected from the observed influence of crowding on the polymer dynamics, these effects were higher at lower protein concentrations (Fig. 7*A*, *closed triangles*). The turnover rate of GTP exchange in the crowding-induced FtsZ ribbons was measured by a pulse-chase experiment with radioactive nucleotide. The results show that the turnover rate in the ribbon (14 s) is slower than in the filaments (≤3 s) (Fig. 7*C*). Surprisingly, GTP exchange already occurred in the ribbon even during the period in which no significant GTPase activity was observed (Fig. 7). This result would be compatible with the exchange of the nucleotide taking place by dissociation of the non-hydrolyzed GTP throughout the polymer.

DISCUSSION

We have established a set of experimental conditions that simulate the physiological bacterial intracellular environment more closely than commonly used standard *in vitro* conditions. This is a novel approach to study bacterial cell division at the molecular level. Atomic force microscopy shows that under these *in vitro* conditions that mimic the crowded environment

of the cell cytoplasm, FtsZ assembles into one subunit thick ribbons. This process is energy-dependent, because it needs the presence of GTP. Our observations indicate that above certain values of volume occupancy (*i.e.* above a critical concentration of Ficoll or dextran) the formation of FtsZ ribbons is favored throughout the assembly process and that filaments are not the predominant species. Although the Z ring structure has been visualized in the cell either by GFP tagging or by immunofluorescence, attempts to reveal such a structure in thin sections under the electron microscope have not succeeded.[3] However, a two-dimensional polymer, one subunit thick, as the structures observed in Fig. 4, would be very difficult to discriminate in transversal sections observed by electron microscopy when bound to the inner membrane of a bacterial cell.

The alignment of FtsZ filaments to form higher order structures could have been predicted on theoretical grounds (45), but the arrangement in two-dimensional ribbons was unexpected and has several important consequences. If all the subunits within a ribbon were in the same orientation, all of them might be able to establish identical interactions and, therefore, to participate simultaneously in constriction. Moreover, all would have identical surfaces exposed to the medium and, therefore, would be equally able to contact the membrane surface or the cytoplasmic domains of the membrane proteins involved in cell division. Finally, all the subunits in these ribbons would be equally accessible to regulatory factors. This means that the dynamics and the stability of the ring might be controlled at many points (as many as FtsZ subunits) besides the polymer ends. In a three-dimensional polymer, on the contrary, the accessibility of the internal subunits would be severely restricted, and only the subunits in one face of the structure would be able to contact the membrane surface.

A question that is crucial to evaluate the biological relevance of our results is whether there are enough FtsZ molecules in a bacterial cell to fully decorate the transversal perimeter of the inner face of the cytoplasmic membrane and assemble as a ribbon into a Z ring. The mean number of FtsZ molecules per *E. coli* cell has been reported to range from 4,000 (41) to 15,000 (12) in different strains. Let us consider the less favorable assumption. Because the intracellular concentration of FtsZ does not change during the *E. coli* cell cycle (41) the lower number of FtsZ molecules in dividing cells is around 6,000. Because FtsZ polymerization follows a cooperative mechanism (Fig. 2), the FtsZ population in the cell would be distributed into two classes, *i.e.* soluble and polymeric forms (Fig. 8). From the value of C_{fil} (the critical FtsZ concentration for assembly into filaments) measured in this work (1.25 μM) and the lower measurement reported for the intracellular contents of FtsZ (3.5 μM (41)) we can calculate that approximately one-third of the FtsZ protein within a cell should be in the soluble form, whereas the remaining two-thirds might form part of the polymers. Considering an axial spacing between FtsZ monomers of 4.3 nm (see also Ref. 10),[4] and a cell perimeter of ~3 μm, if we assume an average of around 4000 FtsZ monomers in the polymeric form (two-thirds of the total found in dividing cells), this would be enough to encircle the cell around six times, which would be compatible with the structure adopting the form of a ribbon even when considering the less favorable set of assumptions. Using a GFP-FtsZ fusion, Stricker *et al.* (46) calculated that only 30% of GFP-FtsZ is found in the ring. This would be incompatible with a continuous ribbon wider than two monomers encircling the cell. However, there is no evidence to support that the behavior of both GFP-FtsZ and native FtsZ is identical.

Our studies favor that, in the crowded bacterial interior, the two main states of FtsZ tend to be soluble FtsZ and ribbons (see Fig. 8). Within *E. coli*, FtsZ in its GDP-bound state, if present, would have a weak tendency to associate into high order oligomers and a much more reduced tendency to form polymers. However, because the GTP/GDP ratio is high under physiological conditions (47), FtsZ is likely to be found as the GTP-bound form, mainly as FtsZ polymers. This in turn would trigger the assembly into ribbons under crowded conditions. Paradoxically no Z rings are observed in the early stages of the cell cycle (41) implying that prior to Z ring formation the GTP-FtsZ species have to remain soluble in the cytoplasm. Formation of the ribbon *in vitro* can be prevented at any of the stages; for example, *reaction 2* in Fig. 8 does not proceed in the absence of potassium ions (see above; Fig. 3*A*). *In vivo* several mechanisms have been proposed that prevent Z ring formation, among them a mechanism that would avoid assembly in the early stages of the *Bacillus subtilis* cell cycle is the FtsZ sequestering protein EzrA (48, 49), which preferentially binds to FtsZ protomers. EzrA would play a similar role as the assembly inhibitors described for tubulin (*i.e.* stathmin (50)) and for actin (*i.e.* ADF/cofilin (51)) in eukaryotic cells. In *E. coli* there are two specific mechanisms that determine the spatial localization of FtsZ rings and may function by preventing the spontaneous assembly of FtsZ into ribbons: nucleoid occlusion and the *min* system (reviewed in Refs. 52 and 53). Both involve negative regulation and might work by locally inhibiting FtsZ polymerization and ribbon assembly.

Acknowledgments—We are grateful to A. Minton for critically reading preliminary versions of the manuscript, to J. M. Valpuesta for EM analysis, and to C. Alfonso for excellent technical assistance.

REFERENCES

1. Bi, E., and Lutkenhaus, J. (1991) *Nature* **354,** 161–164
2. Vitha, S., McAndrew, R. S., and Osteryoung, K. W. (2001) *J. Cell Biol.* **153,** 111–119
3. Löwe, J., and Amos, L. A. (1998) *Nature* **391,** 203–206
4. Nogales, E., Wolf, S. G., and Downing, K. H. (1998) *Nature* **391,** 199–203
5. de Boer, P. A. J., Crossley, R., and Rothfield, L. I. (1992) *Nature* **359,** 254–256
6. Mukherjee, A., Dai, K., and Lutkenhaus, J. (1993) *Proc. Natl. Acad. Sci. U. S. A.* **90,** 1053–1057
7. RayChaudhuri, D., and Park, J. T. (1992) *Nature* **359,** 251–254
8. Rivas, G., López, A., Mingorance, J., Ferrándiz, M. J., Zorrilla, S., Minton, A. P., Vicente, M., and Andreu, J. M. (2000) *J. Biol. Chem.* **275,** 11740–11749
9. Sossong, T. M., Jr., Brigham-Burke, M. R., Hensley, P., and Pearce, K. H., Jr. (1999) *Biochemistry* **38,** 14843–14850
10. Erickson, H. P., Taylor, D. W., Taylor, K. A., and Bramhill, D. (1996) *Proc. Natl. Acad. Sci. U. S. A.* **93,** 519–523
11. Löwe, J., and Amos, L. A. (1999) *EMBO J.* **18,** 2364–2371
12. Lu, C., Stricker, J., and Erickson, H. P. (1998) *Cell Motil. Cytoskeleton* **40,** 71–86
13. Mingorance, J., Rueda, S., Gómez-Puertas, P., Valencia, A., and Vicente, M. (2001) *Mol. Microbiol.* **41,** 83–91
14. Mukherjee, A., and Lutkenhaus, J. (1999) *J. Bacteriol.* **181,** 823–832
15. Romberg, L., Simon, M., and Erickson, H. P. (2001) *J. Biol. Chem.* **276,** 11743–11753
16. Yu, X.-C., and Margolin, W. (1997) *EMBO J.* **16,** 5455–5463
17. Addinall, S. G., and Holland, B. (2002) *J. Mol. Biol.* **318,** 219–236
18. Record, T. M., Jr., Courtenay, E. S., Cayley, S., and Guttman, H. J. (1998) *Trends Biochem. Sci.* **23,** 190–194
19. Zimmerman, S. B., and Trach, S. O. (1991) *J. Mol. Biol.* **222,** 599–620
20. Ellis, R. J. (2001) *Trends Biochem. Sci.* **26,** 597–604
21. Minton, A. P. (2001) *J. Biol. Chem.* **276,** 10577–10580
22. Herzog, W., and Weber, K. (1978) *Eur. J. Biochem.* **91,** 249–254
23. Suzuki, A., Yamazaki, M., and Ito, T. (1989) *Biochemistry* **28,** 6513–6518
24. Lindner, R. A., and Ralston, G. B. (1997) *Biophys. Chem.* **66,** 57–66
25. Rivas, G., Fernández, J. A., and Minton, A. P. (2001) *Proc. Natl. Acad. Sci. U. S. A.* **98,** 3150–3155
26. Weast, R. C. (1982) *CRC Handbook of Chemistry and Physics, 63rd Ed.*, CRC Press Inc., Boca Raton, FL
27. Lu, C., and Erickson, H. P. (1998) *Methods Enzymol.* **298,** 305–313
28. Scheffers, D. J., and Driessen, A. J. M. (2001) *FEBS Lett.* **25254,** 1–5
29. Leirmo, S., Harrison, C., Cayley, D. S., Burgess, R. R., and Record, M. T. J. (1987) *Biochemistry* **26,** 2095–2101
30. Purich, D. L., Terry, B. J., MacNeal, R. K., and Karr, T. L. (1982) *Methods Enzymol.* **85,** 416–433

[3] J. Mingorance and M. Vicente, unpublished observations.

[4] Oliva, M. A., Huecas, S., Palacios, J. M., Martin-Benito, J., Valpuesta, J. M., and Andreu, J. M. (2003) *J. Biol. Chem.* **278,** 33562–33570.

31. Schuck, P., and Rosmanith, P. (2000) *Biopolymers* **54,** 328–341
32. Wenner, J. R., and Bloomfield, V. A. (1999) *Biophys. J.* **77,** 3234–3241
33. Andreu, J. M., and Timasheff, S. N. (1986) *Methods Enzymol.* **130,** 47–69
34. Moreno-Herrero, F., de Pablo, P. J., Fernández-Sánchez, R., Colchero, J., Gómez-Herrero, A., and Baró, A. (2002) *Appl. Phys. Lett.* **81,** 2620–2622
35. Díaz, J. F., and Andreu, J. M. (1993) *Biochemistry* **32,** 2747–2755
36. Hoenig, M., Lee, R. J., and Ferguson, D. C. (1989) *J. Biochem. Biophys. Methods* **19,** 249–252
37. Lanzetta, P. A., Alvarez, L. J., Reinach, P. S., and Candia, O. A. (1979) *Anal. Biochem.* **100,** 95–97
38. Mukherjee, A., and Lutkenhaus, J. (1998) *EMBO J.* **17,** 462–469
39. Caplan, M., and Erickson, H. P. (2003) *J. Biol. Chem.* **278,** 13784–13788
40. White, L. L., Ross, L. J., Reynolds, R. C., Steitz, L. E., Moore, G. D., and Borhani, D. W. (2000) *J. Bacteriol.* **182,** 4028–4034
41. Rueda, S., Vicente, M., and Mingorance, J. (2003) *J. Bacteriol.* **185,** 3344–3351
42. Hall, D., and Minton, A. P. (2002) *Biophys. Chem.* **98,** 93–104
43. Hall, D. (2002) *Biophys. Chem.* **98,** 233–248
44. Minton, A. P. (1983) *Mol. Cell. Biochem.* **55,** 119–140
45. Herzfeld, J. (1996) *Acc. Chem. Res.* **29,** 31–37
46. Stricker, J., Maddox, P., Salmon, E. D., and Erickson, H. P. (2002) *Proc. Natl. Acad. Sci. U. S. A.* **99,** 3171–3175
47. Neurard, J., and Nygaard, P. (1987) in *Escherichia coli and Salmonella typhimurium: Cellular and Molecular Biology* (Neidhardt, F. C., ed) pp. 445–473, American Society for Microbiology, Washington, D. C.
48. Levin, P. A., Kurtser, I. G., and Grossman, A. D. (1999) *Proc. Natl. Acad. Sci. U. S. A.* **96,** 9642–9647
49. Margolin, W. (2003) *Curr. Biol.* **13,** R16–R18
50. Andersen, S. S. L. (2000) *Trends Cell Biol.* **10,** 261–267
51. Pollard, T. D. (1999) in *Guidebook to the Cytoskeletal and Motor Proteins, Second Edition* (Kreis, T., and Vale, R., eds) Oxford University Press, New York
52. Lutkenhaus, J. (2002) *Curr. Opin. Microbiol.* **5,** 548–552
53. Margolin, W. (2001) *Curr. Opin. Microbiol.* **4,** 647–652